Hybrid Fuel Cell / Gas Turbine Systems

Auxiliary Power Unit

Abstract

Recent interest in fuel cell-gas turbine hybrid applications for the aerospace industry has led to the need for accurate computer simulation models to aid in system design and performance evaluation. To meet this requirement, solid oxide fuel cell (SOFC) and fuel processor models have been developed and incorporated into the Numerical Propulsion Systems Simulation (NPSS) software package. The SOFC and reformer models solve systems of equations governing steady-state performance using common theoretical and semi-empirical terms. An example hybrid configuration is presented that demonstrates the new capability as well as the interaction with pre-existing gas turbine and heat exchanger models. Finally, a comparison of calculated SOFC performance with experimental data is presented to demonstrate model validity.

Introduction

Fuel cell technology continues to mature due to innovations from industry, government, and academia. Electric drive-trains for automotive applications are evolving from early pure battery-powered vehicles to commercially viable combustion engine/battery hybrids, with pure fuel cell buses and automobiles undergoing on-road demonstrations. Stationary power fuel cell systems continue to be installed, proving environmental sensitivity and becoming more capable with regard to reliability, availability and user friendliness. New types of fuel cells, such as the direct methanol fuel cell, are potentially creating new market applications for fuel cells including portable power for lap[top of page] computers and other compact electronics.

This continued progress towards more reliable and cost-effective fuel cells establishes a basis to consider fuel cells in aerospace applications. These applications include electrical power units for commercial aircraft and uninhabited aerial vehicles (UAVs) and also propulsion power for UAVs and other small aircraft. NASA has been using fuel cells for the manned space program since its inception and is currently assessing the feasibility of proton exchange membrane (PEM) fuel cells for its next-generation space launch vehicle. Other space applications for fuel cells such as electrical power for satellites and even planetary in-situ-based electrical power units are also being examined.

As in other applications, aerospace fuel cells may offer reduced criteria pollutant (e.g., NO_X, CO, hydrocarbons) and CO_2 emissions when compared to current aviation electrical power production methods. In addition, noise may be diminished as a result of the lower gas velocities and smaller rotating components of fuel cell systems compared to gas turbine combustion engines. Another benefit is that the thermal efficiency of small fuel cell systems is typically much higher than similarly sized aeronautical gas turbines. Any fuel weight saved due to improved efficiency will thus counteract the weight increase due to the lower specific power (power/weight) of fuel cell system compared to the gas turbine. Based on initial analyses, this balance of increased hardware weight versus increased fuel efficiency appears to be one of the primary issues for the design of the system. Moreover, the relative value of hardware weight or fuel efficiency is entirely mission-dependent. The longer the mission, the more fuel weight is saved due to efficiency improvement. While this type of design trade-off is relevant for all forms of transportation, its importance is greatest for aerospace applications. As a result, aerospace fuel cells may ultimately require fuel cell and system designs that differ from that of the ground-based applications.

Fuel cells may also enable new aerospace missions that were previously not possible. An example of such is the reversible-regenerative fuel cell power system, where a complete energy cycle is created to enable extremely long-duration missions. For this system, a fuel cell is combined with an electrolyzer such that hydrogen and oxygen react to form water and electricity in the fuel cell while water is electrolyzed to re-form hydrogen and oxygen in the reverse process. The power required to electrolyze the water comes from an external source such as solar power, a technology that is often used in the aerospace industry.

NASA, along with the fuel cell and aerospace industries, the U.S. Departments of Energy and Defense, and academia (including the National Fuel Cell Research Center at the University of California, Irvine), has begun investigating fuel cells for both UAVs and commercial aircraft. PEM fuel cells are attractive for these applications due to their high specific power when compared to other fuel cell types. In addition, with PEM fuel cells being the primary choice for automotive applications, there is substantial research both in the public and private sectors on this technology resulting in high expectations for commercially viable technology development. However, the PEM fuel cell is very sensitive to fuel impurities (especially carbon monoxide) and when integrated into systems using hydrocarbon fuel sources typically has a lower efficiency than other fuel cell types.

The higher temperature ceramic-based SOFC tolerates fuel impurities and can utilize carbon monoxide as a fuel. In addition, the high temperature operation allows systems design that well uses the fuel cell thermal output, which leads to higher system efficiency than comparable PEM fuel cell systems. For a SOFC, liquid hydrocarbon fuels, including the aeronautical fuels, are much easier to use due to the relaxed constraints on the fuel cell anode inlet gas. The liquid fuels are more energy dense per unit volume than hydrogen, which is also important, especially for longer missions and larger aircraft.

Due to the importance of efficiency and due to the need to operate fuel cells at altitude, the hybrid SOFC/gas turbine cycle is a potentially attractive option for aerospace applications. The myriad of potential fuel cell system designs, configurations, and operating conditions must be analyzed systematically for each mission, as the best system is likely to be different depending on the application. These complexities reinforce the need for systems analysis and optimization tools, such as those presented in this paper, as an element of the overall design process.

Part of the challenge of modeling fuel cell systems is the multidisciplinary nature of the physics and chemistry that governs their performance. Electrochemistry, fluid mechanics, materials science, and electrical engineering, among other disciplines, are all critical to understanding and designing fuel cell systems. In addition, few commercial software packages contain the requisite models for simulating all components of a fuel cell system. Even fewer modeling programs include robust and fundamentally sound strategies for simulation of fuel cells. As a result, new models must be developed.

There have been multiple published approaches to SOFC/gas turbine hybrid models. Massardo and Lubelli [1] developed a primarily theoretical model for a SOFC/gas turbine hybrid that can accommodate equilibrium-based internal methane reforming as well as more typical external fuel reforming (also at equilibrium). The model is used to examine several valuable parametric trends including fuel cell pressure and gas stream temperatures as well as four overall configurations. Later this model is expanded, improved and applied to SOFC/micro-gas turbine [2] and SOFC/personal turbine [3] hybrid systems. Both design and off-design characteristics are included in [2] and [3], with an off-design scheme that takes advantage of the fuel cell performance at off-design and a variable speed gas turbine. In another approach, Burer et al. [4] presents a SOFC/gas-turbine hybrid as one subset of a larger power, heating, and cooling cogeneration system model. Palsson, et al. [5] developed a two-dimensional planar SOFC model to add further fidelity and flexibility to the system and proceeded to evaluate several novel concepts, including networked SOFC stacks [6]. Even ground-based mobile applications using hybrid SOFC/gas turbines have been examined, presented by Winkler and Lorenz [7]. Few published models have been validated at the system level because of the lack of available systems-level data. One study,

produced by Yi et al. [8], has compared the results of a SOFC/gas turbine hybrid model to an operating 220 kW hybrid system.

While these models have been recently developed and used to simulate various applications, no model has been developed with aerospace applications as its focus. Data such as atmospheric conditions at various altitudes and the need for propulsor models require specialized tools that differ from those used in the automotive and stationary power industries. The current effort therefore develops a separate SOFC/gas turbine hybrid model within an existing aerospace code, known as the Numerical Propulsion Systems Simulation (NPSS). This software package is a NASA and U.S. aerospace industry-developed tool used primarily for gas turbine and rocket engine simulation [9,10] .

NPSS is mainly a steady-state zero-dimensional thermodynamic analysis code that was created so that the aerospace community would have a similar tool for aerospace propulsion analysis. In addition to the altitude data and propulsor models, the NPSS code was chosen for this work because of its familiarity and regular use within the aerospace industry. NPSS also contains other aerospace-specific features including a form of the JANNAF thermodynamic data and the Chemical Equilibrium with Applications (CEA) code, developed by Gordon and McBride [11]. CEA is based on the concept of Gibb's Free Energy minimization and can contain a large thermodynamic database of chemical species including thermodynamic information on various types of jet fuel. NPSS also contains built-in gas turbine and heat exchanger components that are readily applicable to the SOFC/gas turbine hybrid system. The compressor and turbine components are capable of both design and off-design analysis with the use of performance maps or other correlations. The heat exchanger is a gas-phase model based on either an input effectiveness or total heat flow.

NPSS also includes a nonlinear system of equations solver that is based on the modified Newton-Raphson method. The solver gives the code remarkable flexibility to balance a system in a number of different ways. Examples include the ability to equalize the compressor and turbine work or, in the case of a reformer, to create an autothermal enthalpy condition.

Nomenclature

Symbol	Units	Description
A	$k\Omega*cm^2$	Pre-exponential factor in resistance equation
E	K	Exponential factor in resistance equation
F	C/mol	Faraday's constant
H_2O/C	-	Molar steam-to-carbon ratio
HX	-	Heat Exchanger
i	mA/cm^2	Current density
i_L	mA/cm^2	Limiting current density
i_n	mA/cm^2	Internal current density
i_o	mA/cm^2	Exchange current density
n	-	Number of electrons transferred per mole of reactant
O/C	-	Molar oxygen-to-carbon ratio
P	Watts	Power
p	kPa	Pressure
pp	-	(as a prefix) partial pressure
$\dot{Q}$	Watts	Heat
r	$kW*cm^2$	Bulk internal area specific resistance term (combines both ionic and electronic resistances)
R	J/K*mol	Universal gas constant
T	K	Temperature
U	-	Overall stack utilization
V	-	Voltage
$\Delta_f G°$	J/mol	Change in Gibb's energy of formation at standard pressures, a function of temperature.
$\Delta\dot{H}$	J/sec	Enthalpy flow (enthalpy times mass flow)
$\dot{N}$	mol/sec	Molar flow rate
α	-	Empirically derived charge transfer coefficient
η	-	Efficiency

Model development

Solid Oxide Fuel Cell (SOFC)

The SOFC model developed in this study is a bulk model that predicts overall performance of a SOFC and utilizes fundamental understanding of fuel cell electrochemistry to predict these outputs. There are no model features that relate to geometry except for the physical cell area, and there are no constraints on the size or physical configuration. This provides a widely adaptable model without the expense of detailed internal flow field, heat flux, and electrochemistry information, each of which is highly dependent on the geometrical configuration of an individual fuel cell stack.

The accuracy of the model therefore comes directly from the integrity of the multiple input values as determined by comparison to experimental results. Default values for the parameterization of the model come from literature sources as accepted generic SOFC performance parameters [12, 13]. The user can retain these default values and run simulations for the purpose of seeing the performance of a typical SOFC stack in various hybrid systems and flight situations. If a user has a detailed SOFC model or an actual SOFC stack, the model parameterization (input values) can be changed to represent the outputs of the detailed model or the measured performance values. This implies that with the correct parameterization (inputs) this model can be used to accurately predict the performance of a system that uses any of the different types and configurations of actual SOFCs being studied today, including both tubular and planar designs.

Many of the thermodynamic and flow calculations (i.e., mass and energy balances) that govern fuel cell operation as predicted by the current model are solved by the NPSS software utilizing the built-in CEA equilibrium model and the numerical solver. The electrochemical and purely electrical equations are added to the built-in structure and are presented below.

The reversible (Nernst) voltage is:

$$V_{rev} = -\frac{\Delta_f G^{\circ}}{nF} + \frac{RT}{nF}\ln\frac{ppH_2 * (ppO_2)^{\frac{1}{2}}}{ppH_2O} \quad , (1)$$

where stack temperature (T) is a user input and is assumed constant throughout the stack, and $\Delta_f G°$ is determined for this temperature for the formation of gaseous water, from the data in the JANNAF tables. *R* is the universal gas constant, *n* is the number of electrons participating in the electrochemical reaction, *F* is Faraday's constant and *pp* is partial pressure. Also, the default partial pressures of the reactants and products used in the Nernst equation are determined at the stack exit. The user can also choose to calculate the Nernst potential using the average partial pressures across the stack, which will give a slightly higher reversible voltage than that of equation (1) using exit partial pressures.

The irreversible voltage losses are due to a number of chemical, physical, and electrochemical processes. In the current approach, these losses are estimated by three overall primary fuel cell losses (or polarizations) (1) activation, (2) ohmic, and (3) concentration. These irreversible voltage losses are determined by [12]:

$$V_{Activation} = \frac{RT}{n\alpha F}\ln\left[\frac{i + i_n}{i_o}\right] \quad , (2)$$

for the activation loss,

$$V_{Ohmic} = r * (i + i_n) \quad , (3)$$

for the ohmic loss, and

$$V_{Concentration} = -\frac{RT}{nF}\ln\left[1-\frac{i+i_n}{i_L}\right], \quad (4)$$

for the concentration loss.

In equations (2)-(4) i represents stack current, i_n the internal current density, i_o the exchange current density, and i_L the limiting current density. Each of the current density terms are defined and explained further within [12]. The bulk internal resistance term, r, can be specified as a constant or can be made dependent on temperature for each stack component (anode, cathode, electrolyte, and interconnect) in a relationship of the form [13]:

$$r = \Sigma r_{Component} = \Sigma A e^{E/T}. \quad (5)$$

Operating voltage is determined by the following:

$$V_{oper} = V_{rev} - V_{Activation} - V_{Ohmic} - V_{Concentration}, \quad (6)$$

and stack power is determined by multiplication of the operating voltage, current density, and total stack active area as follows:

$$P_{Stack} = \frac{V_{Oper} * i * Area}{1000}. \quad (7)$$

Because the NPSS package calculates the flow stream enthalpies at each state in the model, the heat generated by the fuel cell stack reactions is calculated by:

$$\dot{Q}_{Gen} = \Delta\dot{H} - P_{Stack}. \quad (8)$$

where ΔH is the difference in inlet and outlet stream enthalpy flows as calculated by NPSS.

Two efficiencies are calculated, the overall stack efficiency, and the electrochemical efficiency. It is important to separate these two efficiencies for cases when it is desired to optimize stack electrochemical performance. Overall stack efficiency is:

$$\eta_{Overall} = U * \frac{P_{Stack}}{\Delta\dot{H}}, \quad (9)$$

where the overall stack fuel utilization (U) is given by:

$$U = \frac{\Delta_{(IN-OUT)}(\dot{N}_{H_2} + \dot{N}_{CO} + 4\dot{N}_{CH_4})}{(\dot{N}_{H_2} + \dot{N}_{CO} + 4\dot{N}_{CH_4})_{IN}} \quad (10)$$

where $\dot{N}_i$ represents molar flow of species i.

Electrochemical efficiency is defined as:

$$\eta_{Electrochem} = \frac{V_{oper}}{V_{rev}}. \quad (11)$$

Stack temperature and current density are typically input by the user. However, the built-in solver routines enable the user to substitute other variables for the inputs, and solve the model iteratively. For example, current density can be varied until the operating voltage reaches a specified value.

The solver capability of NPSS also enables the SOFC model to accommodate the internal reforming reactions (shown for methane below, but applicable to any hydrocarbon fuel, including jet and diesel fuels):

$CH_4 + H_2O \; CO + 3H_2$ (12)

and the water-gas shift reaction:

$CO + H_2O \rightarrow CO_2 + H_2$. (13)

As water is produced and hydrogen is consumed at the anode, the reforming and shift reactions are driven to produce more hydrogen. Because the model does not simultaneously solve the above system of equations, the complete solution of the concurrent internal reformation and water gas shift reactions and electrochemical oxidation cannot be reached in one step. Multiple steps or iterations are used, where first hydrogen is consumed and water is produced, then the reforming and shift reactions are allowed to occur. This process is repeated until the overall stack utilization matches the user's requirement.

It should also be noted that this ability to consider the water-gas shift reaction enables the direct electrochemical oxidation of CO to be ignored in the determination of electrical power or heat output. This is justified since the fraction of CO being directly electrochemically oxidized by the fuel cell is understood to be small compared to the amount consumed by the water-gas shift reaction, as long as the fuel isn't primarily CO [14].

There are two especially useful methods for the solution of the SOFC model equations. In the first method, the desired power output is specified, and a stack size is calculated based on the specified cell parameters and calculated performance. In the second method, the stack size is specified and the power output performance is calculated. This dual-mode solution strategy allows the user to design a virtual fuel cell stack to meet a set of requirements (for example, 50 kW of power at 1000°C). Then one can subject this specific stack to another set of operating conditions and determine off-design performance (for example, at 1100°C the same stack might generate 55 kW).

Reformer

The reformer model is based on chemical equilibrium, modeled using the CEA program described above. Inputs to the reformer model include the in-flow thermodynamic data such as temperature, pressure, and chemical species compositions, and the desired out-flow temperature and pressure. The model calculates the out-flow chemistry and change in other thermodynamic properties such as enthalpy, entropy, and free energies. The reactants are typically specified by the user using industry-standard quantities, such as the molar steam-to-carbon (H_2O/C) and oxygen-to-carbon (O/C) ratios. The corresponding water and air mass flows are then calculated within the program based on the moles of carbon in the fuel flow (which is typically varied to satisfy a fuel cell power requirement). In addition, H_2O/C and O/C can be varied to satisfy a certain enthalpy change requirement, such as a true autothermal mixture, where the net change in enthalpy is zero. Due to the zero-dimensional nature of the model, the temperature and pressures are assumed to be global values. Finally, pressure drop and heat loss in the reformer can be input as a constant or a function as desired.

More detailed reformer systems can be created using the current model as a basis. Multiple steps in series at different temperatures or integrated heat exchanger/reformer designs that simulate indirect internal reforming with an SOFC have been simulated using the current simulation tool. In addition, validated chemical kinetics-based reformer models would add further accuracy and detail including the capability for spatial and/or transient models.

Model Comparison to Experimental Data

With attention to the experimental conditions and assumptions, the SOFC model can compare well with experimental data. Several sources of data are used to parametrically isolate three important parameters: pressure, temperature, and anode inlet fuel composition. The pressure variation data is from a Siemens Westinghouse tubular SOFC, where voltage vs. current density is recorded for pressures ranging from 1 atm to 15 atm using pure hydrogen fuel [15]. The impacts of temperature and anode inlet fuel composition on SOFC performance are assessed by comparison to single "button" cell SOFC data from the Department of Energy Pacific Northwest National Laboratory[16]. For the temperature variation, the global SOFC temperature is varied from 650°C to 800°C. The anode inlet fuel composition is varied

from 10% H_2 to 97% H_2, with 3% H_2O, and the remainder being N_2 in a separate dataset. Voltage and current density are recorded in both cases.

Pressure Variation

SOFC performance improvement with pressure has been demonstrated by a variety of sources including Siemens Westinghouse. The majority of the improvement is due to the increased partial pressure terms within the Nernst potential equation. However, as Virkar, Fung, and Singhal argue [15], the experimental data suggests that there is also a positive effect on both concentration polarization and, to a lesser extent, activation polarization. This is most likely due to pressure effects on mass diffusion, which is not included in this model. The initial comparison of model predictions to the experimental data of Siemens Westinghouse is shown in Figure 1 based on the known experimental parameters. The anode chemistry is 89% H_2 and 11% H_2O at 85% utilization. The cathode is fed with 6 times the stoichiometric requirement of air. The temperature of the stack is 1000° C.

From Figure 1, the agreement is good for the 1 atm case and in general, at low current densities. However, at higher pressures and higher current densities, the differences are more pronounced. This is because the relative level of concentration polarization increases with current density and therefore the pressure effect on concentration polarization in this region becomes substantial. At each higher pressure the disparity becomes larger. To account for the known impact of pressure on mass diffusion [17] and to account for the experimental observations that suggest a dependence of concentration polarization on pressure, the model was modified to include a variable limiting current density, i_L, as follows:

$$i_L = i_L' * \left(\frac{P}{P'} \right)^a \quad (14)$$

where *a* is a constant, *Pp*_is pressure, and "primed" variables are for atmospheric conditions.

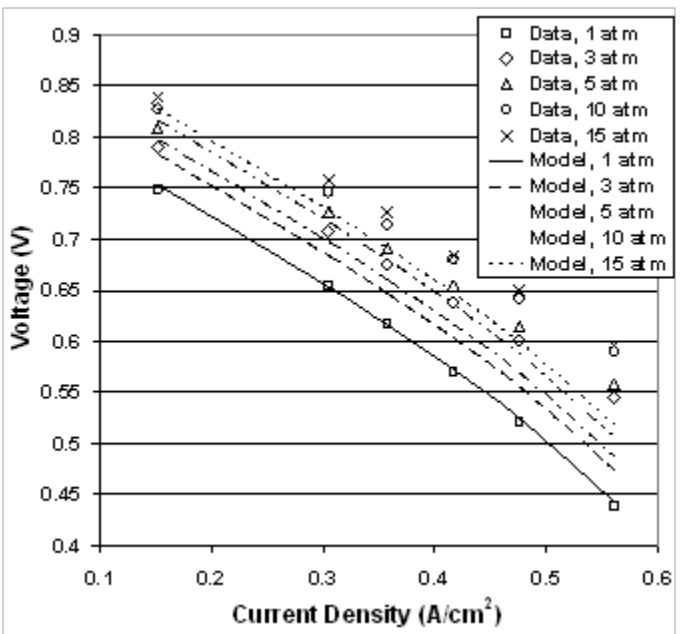

Figure 1. Initial comparison of experimental data with model, parametric pressure variation with constant i_L.

Figure 2 shows a comparison of the modified model to data, which shows very good agreement throughout the test regime. For the simulations presented in Figure 2, a value of 0.35 is used for *a* in equation (14). This results in i_L = 650 mA/cm² and 1677 mA/cm² for pressures of 1 and 15 atm, respectively. This comparison to experimental data shows not only a limitation of the base model, but also the strength of model flexibility that can readily capture observed fuel cell performance. Diffusion limitations are clearly important to capture for certain operating conditions and a complete model should include simulation of such characteristics. An even better match may be possible by varying other SOFC parameters, such as exchange current density (equation (2)), along with i_L, but this is not explored

here. Nonetheless, Figures 1 and 2 demonstrate that the existing model is flexible and simple enough to successfully match experimental SOFC performance versus operating pressure with relative ease.

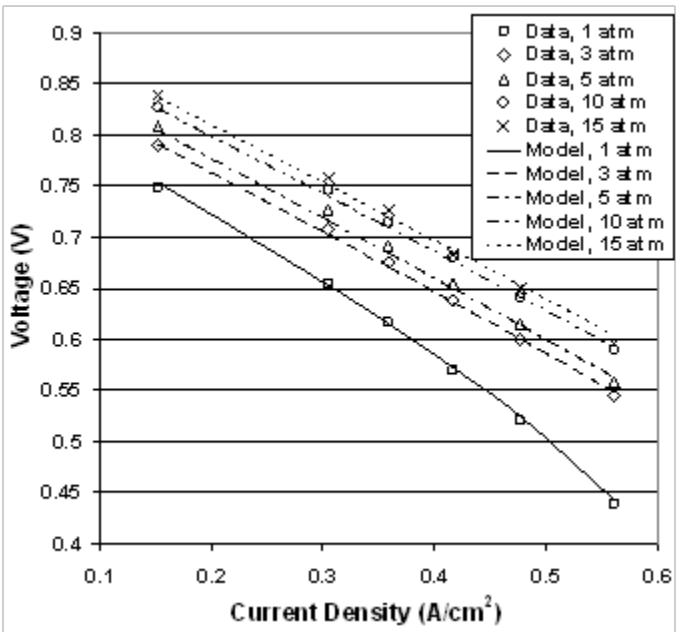

Figure 2. Final comparison of experimental data with model, parametric pressure variation with variable i_L.

Temperature Variation

Understanding fuel cell performance as a function of operating temperature, along with pressure (analyzed above), is required for analysis and design of fuel cell systems. Even though an actual fuel cell can have a substantial (and potentially problematic) temperature gradient, the choice of a desired nominal temperature is an important system parameter that will determine the materials available for the designer as well as the performance of other components. Thus, it is important to accurately capture the affect of fuel cell temperature on the system operation. An important effect of temperature is the corresponding change in cell resistance, which can be modeled using equation (5).

Figure 3 presents a comparison of the model to data of PNNL, where the comparison of model to experimental data is very good except in the extreme region of low temperature and low current density. Since properties such as anode and cathode thicknesses are not known for the experimental fuel cell, bulk values of A = $2.1'10^{-6}$ $k\Omega*\chi\mu^2$ and E = 10,000 K are used in equation (5). As in the pressure study, including the temperature dependence of other SOFC parameters may result in better agreement with experimental data.

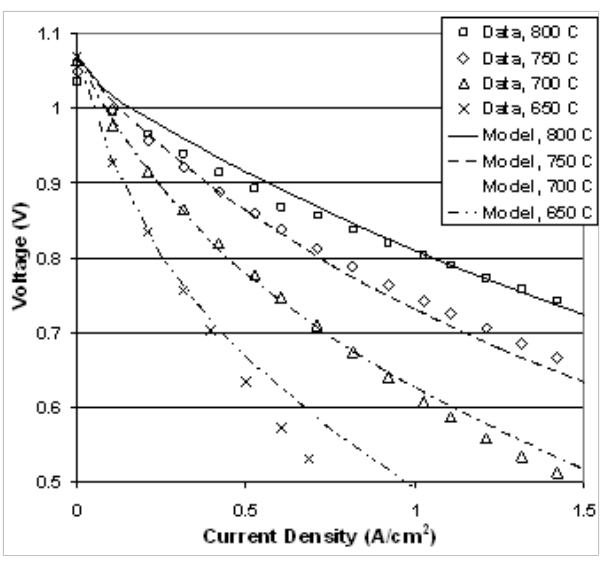

Figure 3. Comparison of experimental data with model, parametric temperature variation.

Anode Inlet Chemistry Variation

The final comparison of the SOFC model to experimental data is a parametric study of anode inlet composition. At higher current densities the anode concentration polarization becomes dominant due to the lack of fuel at the geometrical extremes of the fuel cell. In the cathode, the problem is not as pronounced because typical SOFC operation requires many times the amount of air needed for stoichiometric conversion, primarily for cooling purposes.

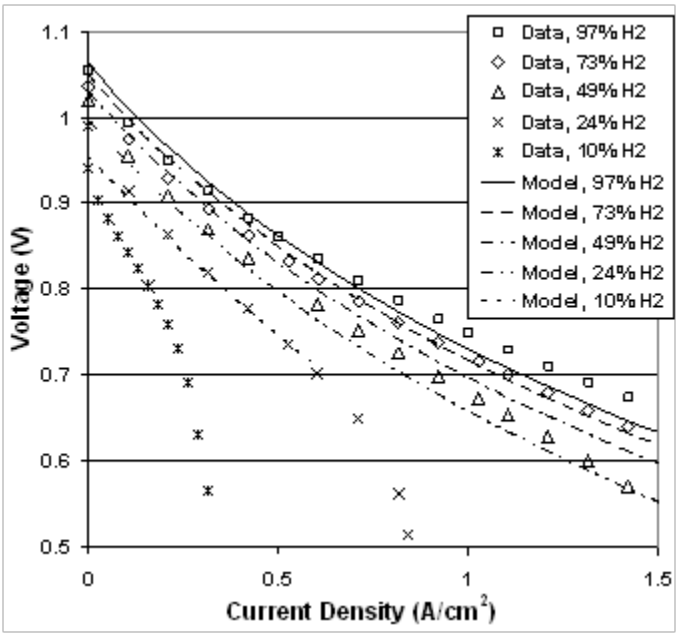

Figure 4. Initial comparison of experimental data with model, parametric composition variation with constant i_L.

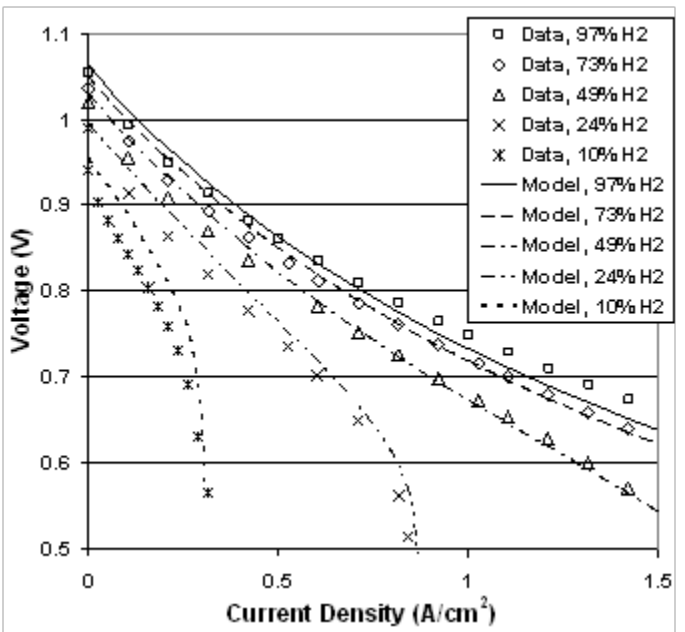

Figure 5. Final comparison of experimental data with model, parametric composition variation with variable i_L.

Since the diffusion-based losses of concentration polarization become the major issue, the initial comparison presented in Figure 4 is similar to the pressure variation comparison of Figure 1. Figure 5 subsequently presents the effect of changing i_L on the overall match between model and experimental data. While no empirical correlation such as equation (14) is presented for variation, values from i_L = 325 mA/cm^2 to 7000 mA/cm^2 are used for anode inlet chemistry from 97% H_2 to 10% H_2, respectively. With the current model level of detail, predicting performance at all conditions may be challenging. However, using experimental data to develop semi-empirical correlations for model parameters and then using the resulting model for systems studies is relatively simple. As in the previous cases, it is possible

that other fuel cell parameters are affected by anode inlet composition, but in this example only the effects on i_L are explored.

SOFC/Gas turbine Hybrid example

Description

A SOFC/gas turbine hybrid system is presented to examine the capability of the models when combined to simulate a hybrid system. (The system is not specific to a particular design or to one aerospace application, but is a general hybrid system design. In addition, the system has not been optimized for efficiency, simplicity, or low cost.) The configuration, as shown in Figure 6, consists of an SOFC, steam reformer, compressor, turbine, and several heat exchangers and pumps. Liquid water is first evaporated and then mixed with the fuel within the steam reformer. For this simulation, the fuel is Jet-A, a kerosene-type jet fuel used for large commercial aircraft. Actual Jet-A is a mixture of many hydrocarbons, but within the CEA thermodynamic database, it is simulated using a carbon-to-hydrogen ratio of 12/23 ($C_{12}H_{23}$). Other properties of Jet-A, such as enthalpies of the liquid and gaseous state, are also included in the database. The reformer parameters, including H_2O/C, are chosen to prevent coking and to maximize the H_2 concentration. The resulting reformate, primarily H_2 and CO, is sent to the anode of the SOFC. The reformer and SOFC temperatures are chosen to be 900 °C for the current simulation, eliminating the need for an additional heat exchanger. The cathode airflow is first pressurized by the compressor to 5 bar and then heated to 900 °C. An estimated pressure drop of 10% in each heat exchanger is assessed such that the inlet SOFC cathode pressure is 4.5 bar. The reformer is also set at this pressure such that the SOFC does not see any differential pressure between the cathode and anode. The combined cathode and anode exhaust is sent through a combustor such that the fuel that remains in the anode off-gas is burned. The fuel utilization is fixed at 75% for this case, although it could be varied to converge on a desired SOFC/turbine power split.

As shown in Figure 6, the combustor exhaust enters the air and water heat exchangers consecutively as the hot gas source. After these heat exchangers, the gases are sent through a turbine, which is designed to expand the gas as much as possible without condensing the water or expanding beyond atmospheric pressure. Any excess turbine power is assumed to produce electricity via a generator operating at 90% efficiency.

The fuel cell input properties are chosen primarily using the defaults as described above and shown in Table 1.

Table 1. SOFC input properties for example SOFC/gas turbine hybrid model shown in Figure 6.

i	500 mA/cm^2
i_L	900 mA/cm^2
i_n	2 mA/cm^2
i_o	300 mA/cm^2
α	1.68
r	0.5 Ω·cm^2

As the steam reforming is an endothermic process, heat is needed to sustain the reactions. For the design of Figure 6, an aggressive indirect internal reforming scheme is used, where some of the SOFC heat produced is used to sustain the reformer reactions. In other words, the reformer is assumed to be thermally integrated into the SOFC stack. A minor amount of direct internal reforming is also used, since some methane remains in the reformate. The remaining heat from the SOFC is assumed to be transferred to its exhaust gases, with the majority of the heat being transferred to the cathode exhaust because of its much higher mass flow rate. Finally, 5% heat loss to the environment is assumed for the combustor, reformer, and SOFC components to simulate more realistic, non-adiabatic behavior.

For this example, the air mass flow rate is determined with the solver such that the overall temperature change through the fuel cell (operating at a nominal 900°C) is at or below 150°C. The fuel flow rate is determined by the electrical power required of the system and is also found using the solver. The water flow rate is determined by the H_2O/C parameter, which is a function of the fuel flow rate.

The final configuration is designed to run at 200 kW net electrical power from the sum of fuel cell and generator power outputs.

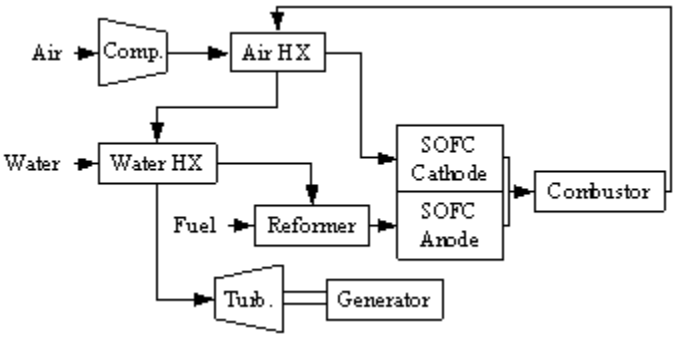

Figure 6. Example SOFC/gas turbine hybrid model.

Results and Discussion

Table 2 lists some of the primary results from the hybrid simulations. The overall thermal efficiency of the system (output electrical power divided by input fuel energy flow higher heating value) is calculated to be 40.6%. SOFC operating voltage for the system was calculated to be 0.571 V at a current density of 500 mA/cm^2. The area specific resistance, *r*, is the dominating polarization term, which is typical for SOFCs, leading to ohmic polarization losses of 0.251 V. Also, the combustor exit temperature is high enough that the first heat exchanger may have to be designed with more exotic materials, which will affect the overall cost of such a system. However, further analysis suggests that the combustor exit temperature could be lowered to a range that more common materials could tolerate. Increasing the SOFC fuel utilization, for example, creates a leaner combustion mixture leading to a lower exit temperature.

Table 2. Simulated performance of the SOFC/gas turbine hybrid model shown in Figure 6.

SOFC net electrical power	186 kW	System thermal efficiency	40.6%
Generator net electrical power	14 kW	SOFC electrochemical efficiency	64.9%
Total net electrical power	200 kW	Compressor adiabatic efficiency	75.0%
Fuel flow	0.0115 kg/s	Turbine adiabatic efficiency	85.0%
Water flow	0.0179 kg/s	Air HX effectiveness	70.2%
Air flow	0.467 kg/s	Water HX effectiveness	69.1%

SOFC

Cell Voltage	0.571 V	Open circuit voltage	0.948 V
Current density	500 mA/cm^2	Nernst voltage	0.878 V
Power density	285 mW/cm^2	Ohmic loss	0.251 V
Utilization	75%	Activation loss	0.0154 V
Temperature	900°C	Concentration loss	0.0412 V
Pressure	4.5 bar	Air stoichiometric ratio	4.0

Reformer

H2O/C	1.2
O/C	0
Temperature	900°C
Inlet pressure	4.5 bar

Combustor

Inlet temperature	1049°C
Exit temperature	1290°C
Inlet pressure	4.3 bar

Compressor

Pressure ratio	4.94
Exit temperature	243°C

Turbine

Pressure ratio	3.35
Inlet temperature	650°C
Exit temperature	446°C

Summary and Conclusions

Solid oxide fuel cell and reformer steady-state models are developed and presented within the NPSS aerospace modeling platform. The SOFC model is compared to experimental data as a function of pressure, temperature, and anode inlet composition variations. The comparisons well validate the capabilities of the SOFC model for predicting fuel cell performance as a function of design specifications and operating conditions. In addition, the comparisons show the ease with which suitable values for

model parameters can be determined and implemented. An example hybrid SOFC/gas turbine system is presented with simulated performance results that demonstrate the capability of the models.

The NPSS modeling tools are currently being used for hybrid configuration design and parametric studies of the key hybrid parameters. Several aerospace applications of such hybrid systems are being analyzed including electrical power units for commercial aircraft and UAVs. Electrically-powered propulsion is also being analyzed as a longer-term objective. The tools developed, validated and applied in the current paper are important tools for potential use in the design and operation of hybrid fuel cell gas turbine systems for aerospace applications.

Personnel

Investigators: J. Brouwer, and G.S. Samuelsen

Students: Joseph W. Pratt

Sponsors

Boeing

NASA

Acknowledgments

The authors appreciate and acknowledge the use of button cell SOFC data versus operating temperature and anode inlet composition acquired by the Pacific Northwest National Laboratory, a laboratory within the U.S. Department of Energy.

References

1. Massardo, A. F. and Lubelli, F., 2000, "Internal Reforming Solid Oxide Fuel Cell-Gas Turbine Combined Cycles (IRSOFC-GT): Part A - Cell Model and Cycle Thermodynamic Analysis," J. Eng. Gas Turbines and Power, **122**, pp. 27-35.

2. Costamagna, P., Magistri, L., Massardo, A.F., 2001, "Design and part-load performance of a hybrid system based on a solid oxide fuel cell reactor and a micro gas turbine," J. Power Sources, **96**, pp. 352-368.

3. Magistri, L., Costamagna, P., Massardo, A.F., Rodgers, C., McDonald, C.F., 2002, "A Hybrid System Based on a Personal Turbine (5 kW) and a Solid Oxide Fuel Cell Stack: A Flexible and High Efficiency Energy Concept for the Distributed Power Market," J. Eng. Gas Turbines and Power, **124**, pp. 850-857.

4.Burer, M., Tanaka, K., Favrat, D., Yamada, K., 2003, "Multi-criteria optimization of a district cogeneration plant integrating a solid oxide fuel cell-gas turbine combined cycle, heat pumps and chillers," Energy, **28**, pp. 497-518.

5.Palsson, J., Selimovic, A., Sjunnesson, L., 2000, "Combined solid oxide fuel cell and gas turbine systems for efficient power and heat generation," J. Power Sources, **86**, pp. 442-448.

6.Selimovic, A. and Palsson, J., 2002, "Networked solid oxide fuel cell stacks combined with a gas turbine cycle," J. Power Sources, **106**, pp. 76-82.

7.Winkler, W., and Lorenz, H., 2001, "The design of stationary and mobile solid oxide fuel cell-gas turbine systems," J. Power Sources, **105**, pp. 222-227.

8. Yi, Y., Smith, T., Brouwer, J., Rao, A., Samuelsen, S., 2003, "Simulation of a 220kW Hybrid SOFC Gas Turbine System and Data Comparison," 203rd Meeting of The Electrochemical Society, Paris, France .

9.Lavelle, T., Felder, J., Butzin, E., 2003, "Using the Numerical Propulsion System Simulation to Model Thermodynamic Systems," JANNAF Joint Subcommittee Meeting, Colorado Springs, CO, USA .

10. Lytle, J., et al., 2003, "2002 Computing and Interdisciplinary Systems Office Review and Planning Meeting," NASA TM-2003-211896.

11. Gordon, S., and McBride, B.J., 1994/1996, "Computer Program for Calculation of Complex Chemical Equilibrium Compositions, and Applications," NASA RP-1311, Parts I and II.

12. Larminie, J. and Dicks, A., 2000, *Fuel Cell Systems Explained*, John Wiley & Sons, England .

13. Gemmen, R. S., Liese, E., Rivera, J., Jabbari, F., Brouwer, J., 2000, "Development Of Dynamic Modeling Tools For Solid Oxide And Molten Carbonate Hybrid Fuel Cell Gas Turbine Systems," 2000-GT-0554, ASME Turbo Expo 2000, Munich, Germany .

14. Weber, A., Sauer, B., Müller, A.C., Herbstritt, D., Ivers-Tiffée, E., 2002, "Oxidation of H_2, CO and methane in SOFCs with Ni/YSZ-cermet anodes," Solid State Ionics, **152-153**, pp. 543-550.

15. Virkar, A.V., Fung, K.Z., Singhal, S.C., 1997, "The Effect of Pressure on Solid Oxide Fuel Cell Performance," IEEE - Region 3 Southeastcon `97 Conference, Blacksburg, VA, USA .

16. Chick, L.A., Williford, R.E., Stevenson, J.W., Windisch, Jr. C.F., Simner, S.P., 2002, "Experimentally-Calibrated, Spreadsheet-Based SOFC Unit-Cell Performance Model," Proceedings of 2002 Fuel Cell Seminar, Palm Springs, CA, USA.

17. Mills, Anthony F., 2001, *Mass Transfer*, Prentice-Hall, Inc., New Jersey, USA .